

Open access • Proceedings Article • DOI:10.2514/6.1985-2018

Electrode erosion in arc discharges at atmospheric pressure — [Source link](#)

T. L. Hardy

Institutions: Glenn Research Center

Published on: 01 Sep 1985

Topics: Electric arc, Plasma arc welding, Anode, Cathode and Electrode

Related papers:

- Cathode degradation and erosion in high pressure arc discharges
- Tungsten electrode erosion on DC horizontal short free arc in air
- Experimental investigation of the anode region of a free-burning atmospheric-pressure inert-gas arc I. General characteristics of the discharge. Low-current regime
- Cathode erosion in high-current high-pressure arc
- Comparison and Evaluation of Electrode Erosion Under High-Pulsed Current Discharges in Air and Water Mediums

Share this paper:    

View more about this paper here: <https://typeset.io/papers/electrode-erosion-in-arc-discharges-at-atmospheric-pressure-26koz6gcdc>

General Disclaimer

One or more of the Following Statements may affect this Document

- This document has been reproduced from the best copy furnished by the organizational source. It is being released in the interest of making available as much information as possible.
- This document may contain data, which exceeds the sheet parameters. It was furnished in this condition by the organizational source and is the best copy available.
- This document may contain tone-on-tone or color graphs, charts and/or pictures, which have been reproduced in black and white.
- This document is paginated as submitted by the original source.
- Portions of this document are not fully legible due to the historical nature of some of the material. However, it is the best reproduction available from the original submission.

Electrode Erosion in Arc Discharges at Atmospheric Pressure

(NASA-TM-87087) ELECTRODE EROSION IN ARC
DISCHARGES AT ATMOSPHERIC PRESSURE (NASA)
21 p HC A02/MF A01

CSCL 21C

N85-34178

G3/20 Unclas
22224

Terry L. Hardy
Lewis Research Center
Cleveland, Ohio

Prepared for the
18th International Electric Propulsion Conference
cosponsored by the AIAA, JSASS, and DGLR
Alexandria, Virginia, September 30–October 2, 1985

NASA



ELECTRODE EROSION IN ARC DISCHARGES AT ATMOSPHERIC PRESSURE

Terry L. Hardy

National Aeronautics and Space Administration
Lewis Research Center
Cleveland, Ohio 44135

Abstract

An experimental investigation was performed in an effort to measure and increase lifetime of electrodes in an arcjet thruster. The electrode erosion of various anode and cathode materials was measured after tests in an atmospheric pressure nitrogen arc discharge at powers less than 1 kW. A free-burning arc configuration and a constricted arc configuration were used to test the materials.

Lanthanum hexaboride and thoriated tungsten had low cathode erosion rates while thoriated tungsten and pure tungsten had the lowest anode erosion rates of the materials tested. Anode cooling, reverse gas flow, and external magnetic fields were all found to reduce electrode mass loss.

Introduction

The direct current arcjet thruster is presently being considered as an auxiliary propulsion device for space applications because of its wide thrust range, high specific impulse capability (400 to 1000 sec), and inherent simplicity. Due to available power and spacecraft interaction considerations near-term applications appear to be at power levels less than 5 kW with ammonia or hydrazine as the propellant. Although arcjets had been investigated in the 1960's, the research was primarily concerned with power levels on the order of 30 kW with hydrogen as the propellant.¹ At 30 kW, two tests were run with hydrogen for over 500 hr at approximately 1000 sec specific impulse with thrust efficiencies greater than 40 percent.^{2,3} At 2 kW, a test was run in hydrogen for 150 hr,⁴ however, tests performed at power levels of 1 kW experienced severe electrode erosion, especially with gases other than hydrogen.⁵ Therefore, a study of electrode erosion at low power levels was required.

Because increased energy efficiencies can be obtained at higher pressure, it is desired to operate arcjets at 1 atm or higher.⁶ Much of the research on electrode erosion in arc discharges has been under vacuum conditions.⁷⁻⁹ Because the electron emission and electrode erosion mechanisms are different in vacuum and atmospheric pressure arcs, the erosion rates are probably also different. Kimblin¹⁰ has done a study on cathode erosion in the transition from vacuum to atmospheric pressure, but copper and graphite were the only materials considered in this study. Cobine and Burger¹¹ present data on anode erosion for various materials in high pressure arcs, but the current level was greater than 11 000 A, which is at least two orders of magnitude greater than the current levels being considered in the low power arcjets.

Therefore, as a continuation of research by Hardy and Nakanishi,¹² the present study addresses the problem of achieving long electrode life (>1000 hr) in low power arcjets by measuring the electrode erosion in a free-burning arc discharge, as well as the erosion in a constricted arc similar to previous arcjet designs. Tests have been conducted to characterize the electrode erosion of various materials in nitrogen at 1 atm at operating powers of 1 kW or less. Also, in an effort to reduce erosion the gas flow direction, electrode cooling, and the number of starts have been examined. Preliminary results of the mass loss of the electrodes in an external magnetic field, used to reduce erosion, are also presented.

Apparatus

The experimental apparatus for the evaluation of electrode erosion is shown in Fig. 1. The test chamber was constructed of pyrex and a roughing pump was used to obtain pressures as low as 0.3 torr. Gas could be fed into the chamber through an external port to increase the pressure. A current-controlled, voltage-regulated dc power supply with a 600 V, 25 A capacity was used with a 0.5 mH, 150 A inductance coil and a variable resistor, normally set at 5 ohm, completing the circuit. Direct current meters were used to read voltages and currents. Due to a power supply malfunction, the 600 V, 25 A power supply was replaced with a 100 A, 100 V power supply for some tests. This supply used an additional 500 V power supply to ignite the arc, and a series-pass linear transistorized current regulator was used in place of the resistors and inductance coil. All gases used were 99.995 percent pure.

Free-Burning Arc

Figure 2 is a schematic diagram of the free-burning or unconstricted arc configuration. This configuration had no confinement of the gas flow. The electrodes were held in place with brass support pieces fabricated to screw into 1.27 cm o.d., 19.1 cm long copper tubes. A ceramic tube 1.91 cm o.d., 19 cm long was placed over the cathode-side copper tube to prevent arc formation on the copper. The anode-side copper tube was fabricated to allow after cooling if desired, and gas could either be fed through the cathode (conventional flow) or over the anode (reverse flow). Boron nitride covers were fabricated for both the anode and cathode to prevent arc formation on the brass holder. A 5.08 cm diameter quartz tube was placed over the electrodes to prevent eroded material from coating the inside of the pyrex test chamber.

Cathodes

Five different cathode materials were investigated using this free-burning arc apparatus:

1. Lanthanum hexaboride tube: Because of promising results from previous tests,^{13,14} a lanthanum hexaboride (LaB_6) tube, 0.53 cm o.d., 0.30 cm i.d. was used. Lanthanum hexaboride has a melting point of 2210 °C. The tube was fabricated by a hot-pressing sintering technique and had a typical density of 80 percent. Because lanthanum hexaboride was found to develop thermal stress cracks upon heating, a supporting tube of molybdenum was placed over the LaB_6 tube with tantalum foil placed between the molybdenum and the LaB_6 to insure a tight fit and good electrical contact.

2. Hafnium Carbide tube: Due to its high melting point (3890 °C), hafnium carbide (HfC) has been suggested for use as cathode material in arcjets.^{15,16} A 0.53 cm o.d., 0.30 cm i.d. tube, hot-pressed sintered from powder, had a typical density of 75 percent. Initial tests showed that this material also developed thermal stress cracks, requiring a molybdenum outer tube for support similar to the LaB_6 configuration.

3. Two Percent Thoriated Tungsten tube: Previous experiments indicated that thoriated tungsten ($\text{ThO}_2\text{-W}$), when operated in an oxygen-free environment, may have a low cathode erosion rate.¹ Thoriated tungsten has a melting point of 3410 °C and the tube used was 0.64 cm o.d., 0.53 cm i.d., with a density of 97 percent.

4. Graphite Rod: Graphite with a density of 87 percent was used in a rod configuration, 0.32 cm diameter, ground flat on three sides to allow gas flow. Graphite sublimes at 3652 °C.

5. Copper Rod: To test the reliability of the cathode erosion measurements, a copper rod, melting point 1083 °C, was used allowing a comparison with data found in the literature. This copper rod was 0.64 cm diameter, ground flat on three sides to allow gas flow.

Anodes

Six different anode configurations were used in this free-burning arc configuration:

1. Water-cooled copper rod, 0.64 cm diameter.
2. Two percent Thoriated tungsten rod, 0.64 cm diameter. This configuration was used both with and without water cooling.
3. Pure tungsten rod, 0.64 cm diameter.
4. Hafnium carbide tube, 0.53 cm o.d., 0.30 cm id.
5. Barium Oxide Impregnated Porous Tungsten tube, 0.53 cm o.d., 0.30 cm i.d.
6. Two percent thoriated tungsten insert, 0.64 cm diameter, 0.10 cm orifice. This insert was fabricated in the shape of a converging-diverging nozzle.

Magnetic Field

Figure 3 is a schematic diagram of the fixed magnet configuration. A 0.32 cm diameter thoriated tungsten rod was used as the cathode and a 0.64 cm diameter thoriated tungsten insert was used as the anode. This anode typically had a 0.10 cm orifice and a 45° nozzle angle. Four rectangular 35 percent Samarium, 65 percent Cobalt magnets, 3500 G at the surface, 1.75 by 1.25 by 0.50 cm, were placed on a steel support to provide the magnetic field. The magnets provided an axial magnetic field of 100 G at the electrodes. A gaussmeter was used to measure the magnetic field strength both before and after the tests. Two boron nitride cylinders were used to isolate the steel support from the copper tubes supporting the electrodes. This configuration was also used without the magnets for comparison purposes.

Constricted Arc

In addition to the free-burning arc configuration, a constricted arc configuration with confined gas flow was constructed to measure erosion in configurations similar to previous arcjet designs. Figures 4 and 5 show the configurations used. Figure 4 is the conventional configuration where the water-cooled copper constrictor acts as the anode with gas flow from cathode to anode. Two anodes were used in this configuration. One anode was a 1 cm diameter copper disk, 0.96 cm thick, with a 0.10 cm orifice to allow flow through the constrictor. The other anode was a 0.64 cm diameter thoriated tungsten insert fabricated in a nozzle configuration. This insert had an orifice 0.10 cm diameter. The thoriated tungsten was pressed into a copper disk 1.00 cm o.d., 0.64 cm i.d., 0.96 cm thick. Both copper disks were fabricated to screw into a brass fitting, which was soldered to the inner copper tube. This copper tube was 1.58 cm i.d. and 0.96 cm long, and was soldered to an outer copper tube 2.70 cm i.d., 7.62 cm long. Copper disks were soldered to the copper tubes to contain the cooling water. The cathodes used in this configuration were a lanthanum hexaboride tube, a thoriated tungsten tube, and a 0.32 cm diameter thoriated tungsten rod, ground flat on three sides to allow gas flow over the cathode. A 2.54 cm o.d. quartz tube was placed inside the outer copper tube to restrict the gas flow. This quartz tube extended from the copper tube to the flange on the pyrex test chamber.

Figure 5 shows the modification to the apparatus shown in Fig. 4. This modification allowed the cathode to be placed in the position of the anode and the gas flow to be from anode to cathode in a reverse flow pattern. In this configuration, a 0.76 cm long LaB_6 tube was placed in a 0.96 cm long molybdenum tube. The LaB_6 tube acted as the cathode and was press fit into a copper disk, which was fabricated to fit into the brass fitting as described previously. Similarly, a $\text{ThO}_2\text{-W}$ tube was used as a cathode. On the downstream end of the cathode, a thoriated tungsten nozzle with a 0.10 cm orifice was pressed into copper disk and fit inside the brass support piece to constrict the flow. The anode was a 0.64 cm diameter thoriated tungsten rod ground flat just enough

(0.02 cm) on three sides to allow gas flow. One boron nitride cover fit against the quartz tube and under the outside copper tubing on the constrictor to prevent gas leakage. Another boron nitride cover was placed over the anode to prevent possible arc formation on the brass supporting the anode, and a third boron nitride disk placed over the cathode tube prevented arcing to the copper constrictor.

Procedure

Arc Characteristics

The arc V-I characteristics were obtained with both argon and nitrogen for various gaps, or distance between the electrodes, for a current range of 5 to 15 A. The arc was started with a voltage of 400 to 500 V with argon at 0.5 to 10 torr background pressure at flow rates 100 to 140 SCCM. After initiation of the arc, the pressure was raised to 760 torr in argon and the arc was allowed to run for 5 min before readings were taken. The first voltage measurement was then taken at 5 A for a gap width of 0.3 cm. Then the current was raised by 1 A, and after 2 or 3 min another measurement was taken. This procedure was repeated for the full range of currents, after which the gap was increased to 1 cm and the voltage measurements were taken as described for a gap of 0.3 cm. After the measurements were taken in argon, the chamber was pumped down to approximately 50 torr, nitrogen was allowed to flow into the chamber from the cathode, and then nitrogen was bled into the chamber from an external port to raise the chamber pressure to 760 torr. The pressure was maintained by drawing a vacuum to offset the flow. The procedure was then repeated as described for argon.

Mass Loss Tests

Measurements were made of the electrode mass loss of various electrode materials tested in high purity nitrogen. Tests were also performed which compared the effects of anode cooling, gas flow direction, and the number of starts on electrode erosion. The mass loss rates in free-burning arc, constricted arc, and magnetic field configurations were compared.

Due to difficulties in starting an arc in nitrogen, argon was used in all tests to initiate the arc. As in the arc characteristic tests, the arc was started with a 400 to 500 V input at 0.5 to 10 torr in argon at 10 A and 0.3 cm gap with flows of 140 SCCM. Once the arc was stable at these pressures, the pressure was raised to 760 torr by back-filling argon into the chamber. After 5 min the argon was shut off, the chamber was pumped down to 50 torr, nitrogen was allowed to flow through the cathode tube at 100 SCCM, and nitrogen was bled into the tank to raise the chamber pressure to 760 torr. This was repeated to insure that the argon was pumped out of the test chamber. In the constricted arc configuration tests, some experiments were performed with a gas flow of 4000 SCCM. In these high flow tests a constrictor chamber pressure of 600 torr was achieved with a background pressure of 10 to 15 torr.

After arc initiation, most tests were run for 2.5 hr, after which the test was stopped and the chamber was allowed to cool 30 to 45 min. The starting and running procedures were then repeated to ensure constant arc conditions. The total run time per experiment was approximately 5 hr. In the tests comparing the number of starts, the arc was initiated 4 and 8 times in a 5 hr period, as opposed to two starts in most other experiments. After the run was completed, the chamber was allowed to cool for at least 1 hr after which the electrodes were removed and weighed on a scale with an accuracy of 0.001 g. The entire test procedure was then repeated with new electrodes and an average mass loss for the two tests was reported. The results are presented as a mass loss per unit time, or a mass loss rate, with error bars representing the span of the electrode erosion.

Results and Discussion

Free-burning Arc

Arc characteristics. Figure 6(a) shows the voltage-current characteristics of a hafnium carbide cathode at different gap widths while Fig. 6(b) shows the V-I characteristics for a lanthanum hexaboride cathode. As was shown in previous tests of a thoriated tungsten cathode,¹² the arc voltage in nitrogen here was 20 to 45 V higher than the arc voltage in argon, a difference attributed to a difference in the plasma properties of the two gases. Also, the voltage decreased as the current was increased. As discussed by Finkelnburg and Maeker¹⁷, as the current increases the conductivity of the gas increases, thus decreasing the electrical impedance and hence the voltage. Finally, as the distance between the electrodes increased, the arc voltage increased. This increase in arc voltage may have been due to an increase in the potential fall across the column, or possibly due to an increase in the anode voltage drop. This effect is important as a change in arc voltage may reflect electrode ablation. It is to be noted that, due to buoyancy forces at gaps larger than 0.5 cm, the actual arc length may have been longer than the measured gap between the electrodes. This effect was reported by Cobine.¹⁸

A separate arc characteristic test was performed using graphite electrodes in N₂. The results obtained were compared with values found in the literature, as shown in Fig. 7. Because the V-I characteristics agree within 3 V of those presented by Cobine,¹⁹ it is assumed that the arc characteristic results obtained for other materials reported herein are valid.

Cathode mass loss. The cathode mass loss for various materials in a nitrogen free-burning arc is given in Fig. 8. Water-cooled copper was chosen as the anode to prevent eroded anode material from being transferred to the cathode, thus affecting the results. The mass loss rate of copper was 3.4x10⁻³ g/min. This result agreed closely with the results of Semenova and Petrova,²⁰ who found the mass loss of copper in nitrogen at 9 A to be 3.6x10⁻³ g/min. Graphite had a mass loss of 8.7x10⁻⁴ g/min. Hafnium carbide had a mass loss rate of 6.6x10⁻⁵ g/min; however, after the 5 hr run, the cathode was examined

and a copper-colored metallic coating was seen on the surface of the hafnium carbide. This coating may have been hafnium nitride, HfN. Thoriated tungsten had a mass loss of 4.1×10^{-5} g/min. Lanthanum hexaboride showed no measurable mass loss to 0.001 g, over the 5 hr test, or a mass loss rate less than 0.33×10^{-5} g/min. In previous tests,¹² lanthanum hexaboride was found to have a mass loss rate of 1.4×10^{-4} g/min. During those previous tests, however, the LaB₆ cathode was run in nitrogen with oxygen impurities. As shown by Futamoto, et. al.,²¹ oxygen may be damaging to lanthanum hexaboride, forming La₂O₃ at the surface. This oxide formation may decrease emission and increase evaporation. For the data shown in Fig. 8 the arc voltages were 38+2 V for HfC, LaB₆, ThO₂-W, and Cu and 60+5 V for graphite.

The mechanism of cathode erosion at high pressures in continuous arcs has yet to be identified. The two significant mechanisms for cathode erosion appear to be evaporation from heating at or near the melting point of the material and sputtering due to ion bombardment.²² Under vacuum (approximately 10^{-5} torr) cathode material is ejected into the plasma column to sustain emission. At atmospheric pressure, however, material may be deposited back onto the cathode due to the high pressure above the surface. As discussed by Kimblin,¹⁰ this effect would result in measured values of erosion being lower at atmospheric pressure than calculated values of evaporation. It has been found, however, that measured erosion rates for refractory materials such as graphite and thoriated tungsten are actually higher than the erosion rates if only evaporation is considered.^{8,12,23} Holm²⁴ suggests on the basis of his calculations that sputtering is the predominant mechanism for erosion at low arc currents. Ion bombardment may dislodge material from the surface of the cathode with enough force to prevent redeposition onto the surface. Unfortunately, little information exists for sputter yields at low ion energies (<100 V). Sputtering due to ion bombardment or a combination of sputtering and evaporation may be the mechanism for cathode mass loss, but further testing to determine sputter yields at low ion energies is required.

Cathode material selection. From measurements of the cathode mass loss (Fig. 8) hafnium carbide, thoriated tungsten, and lanthanum hexaboride appear to be suitable cathode materials. Hafnium carbide has a high melting point; however, formation of hafnium-nitrogen compounds may decrease performance over long periods of time. Thoriated tungsten gave a low mass loss rate, but the cathode spot moved rapidly over the surface of the cathode at 10 A in the free-burning arc configuration. The movement of the spot was more visually evident with thoriated tungsten than with either lanthanum hexaboride, or hafnium carbide. This random movement may be due to localized depletion of thoria, the low work function additive.²⁵⁻²⁷ Tests must be run at low power in nitrogen to determine if depletion of thoria does occur over long periods of time.

Lanthanum hexaboride showed no measurable mass loss when used with a water-cooled copper anode. However, due to its poor mechanical properties

this material required special techniques of support to prevent thermal stress cracks. Therefore, it appears that thoriated tungsten and lanthanum hexaboride are two candidate cathode materials for an arcjet thruster, but long-term tests (>100 hr) must be run to determine the optimum material.

Anode mass loss. The anode mass losses for hafnium carbide, barium-oxide impregnated porous tungsten, thoriated tungsten, and pure tungsten are shown in Figure 9. These tests were performed with a lanthanum hexaboride cathode. Since LaB₆ had the lowest cathode erosion its use was seen as affecting the anode erosion results the least of the materials tested. Hafnium carbide and barium-oxide impregnated porous tungsten had similar mass loss rates at 1.6×10^{-3} and 1.3×10^{-3} g/min, respectively. Thoriated tungsten had a lower mass loss rate at 3.8×10^{-4} g/min while tungsten showed the lowest mass loss rate at 1.8×10^{-4} g/min.

Evaporation appears to be the primary mechanism for mass loss at the anode in a free-burning arc. Hafnium carbide has a high melting point, but its evaporation rate is higher than that of tungsten.²⁸ Impregnated tungsten materials may lose the additives upon excessive heating, causing higher erosion rates.²⁹ Thoriated tungsten gave a mass loss rate higher than that of tungsten, but thoriated tungsten has the advantage of being more easily machined to desired configurations than pure tungsten. Therefore, it appears that thoriated tungsten and pure tungsten are the best anode materials from the evaluation made here with thoriated tungsten being better from the standpoint of machinability.

From the comparison of anode and cathode mass loss rates in the free-burning arc it appears that the anode loss rate is greater than the cathode mass loss rate by at least one order of magnitude at high pressures. At atmospheric pressure, the arc forms a constricted zone, or anode spot, which imposes a severe heat load on the anode. It has been found from previous studies that movement of the arc on the anode surface distributes the heat load, reducing evaporation.^{5,30} One method of moving the anode spot in a free-burning arc is to impose a magnetic field on the arc, which causes the arc to move in a circular motion at high velocities. This method of moving the arc has had success in high current arcs,^{22,31} and further experimentation is required to determine the benefits of using a magnetic field to reduce anode erosion in low power arcs.

Water Cooling Effects. Figure 10 shows the mass loss of a lanthanum hexaboride cathode under different conditions of anode cooling. When using a thoriated tungsten rod anode with no water cooling, the mass loss of the lanthanum hexaboride was 3.2×10^{-4} g/min. When the thoriated tungsten rod was water cooled, the LaB₆ mass loss was an order of magnitude less, and when a copper, water-cooled anode was used the cathode showed no measurable mass loss. The arc voltage for all tests was 38+2 V.

It appears that anode cooling decreased the erosion of the cathode. John, et.al.,²³ found similar results in that the combined anode/cathode erosion rate decreased when a water-cooled anode

was used. This decrease may have been the result of the gas near the cathode being cooled by the anode. The difference between the cathode mass loss with different anode materials may also have been due to a gas cooling effect, as the tungsten had a lower thermal conductivity than copper, and hence, was not cooled as readily by the water. Although water for cooling may not be available for space applications, the results indicate that other, more practical, means of anode cooling, such as regenerative cooling, may improve cathode life.

It must be noted that, without anode water cooling the anode and cathode erosion rates are similar.

Gas flow direction. Figure 11 shows the anode mass loss for two different gas flow directions using a lanthanum hexaboride cathode and a thoriated tungsten anode. The anode mass loss rate for flow from cathode to anode, or conventional flow, was 3.77×10^{-4} g/min with an arc voltage of 38 ± 2 V and the mass loss rate for flow from anode to cathode, or reverse flow, was 1.07×10^{-4} g/min with an arc voltage of 33 ± 2 V. This reduction in mass loss was probably the result of film cooling at the anode surface. The decrease in arc voltage may have been due to a decrease in the anode fall voltage although the effects are still unclear at this time.

Figure 12 shows the cathode mass loss for the two flow directions for a lanthanum hexaboride cathode. The cathode mass loss for conventional flow was 3.28×10^{-4} g/min, while the mass loss for reverse flow was 2.30×10^{-4} g/min. Because the cathode configuration was a tube, the gas flowed through the inside of the cylinder. Therefore, one would expect that conventional flow would have provided more cooling than reverse flow, reducing possible evaporation losses. However, the cathode spot in a high pressure arc forms on the face and outer edge of the tube. Thus, the highest temperatures were at the outside of the tube. Flow from the anode may have increased cathode cooling, reducing the temperature and erosion of the outside of the tube.

Although the mass loss decreased with reverse flow the issues of energy efficiency and arc voltage must be resolved before the results can be applied to an arcjet thruster.

Number of Starts. The effect of the number of starts on cathode mass loss for thoriated tungsten and lanthanum hexaboride is shown in Fig. 13. For a 2 percent thoriated tungsten cathode run for 5 hr in nitrogen, the mass loss rate was 4.1×10^{-5} g/min for two starts, 8.3×10^{-5} g/min for four starts, and 1.67×10^{-4} g/min for eight starts. For a LaB₆ cathode there was no measurable erosion for two and four start tests. Upon removal from the test chamber after the eight start test, the LaB₆ cathode showed evidence of cracking and chipping not seen in the tests with two and four starts. The increase in the number of starts did not have an effect on the appearance of the thoriated tungsten.

The linear dependence of the mass loss on the number of starts for thoriated tungsten indicates a constant depletion of material, possibly thoria,

at the start. The thermal stresses from a large number of starts may cause lanthanum hexaboride cracking, as was seen when the LaB₆ cathode was used without a molybdenum support tube. This cracking may be a major drawback to the use of LaB₆ in a practical thruster design. However, it may be possible to reduce this cracking by using better supports on the LaB₆, thus increasing the ability of the material to withstand the shock imposed by the high voltage start.

It is important to note that by presenting the results as a mass loss rate it is assumed that the mass loss is continuous over a period of time. For certain materials, however, the mass loss may in fact depend more on the number of starts than on the actual run time, as was shown for thoriated tungsten. If this is the case then a mass loss rate is not meaningful. Tests are continuing to determine whether most of the electrode erosion occurs at the start or during the steady-state run.

Magnetic field tests. Imposing a magnetic field on the arc has been found to rotate the anode spot, thus distributing the heat load on the anode to reduce localized melting. Figure 14 shows the anode mass loss for a thoriated tungsten insert with a 100 Gauss axial magnetic field compared to the mass loss in this free-burning arc configuration with no magnetic field. The mass loss with no magnetic field was 7.2×10^{-4} g/min while the mass loss with a 100 G magnetic field was 3.2×10^{-4} g/min. The arc voltage with no magnetic field was 32 V while the arc voltage with the applied field was 37 V. The arc moved randomly over the surface of the cathode in the test with no magnetic field, and an anode spot was visible. With a 100 G field, no anode spot was visible and the arc appeared diffuse compared to the thin filament arc seen without magnetics. Also, the arc stayed on the tip of the cathode during most of the 5 hr test, although some random movement did occur. It was not known if the diffuse arc seen was actually a rapidly spinning anode spot or whether the attachment was actually diffuse at the anode surface. No apparent loss of magnetic field was seen from gaussmeter readings taken after the tests. Deposits from the anode were seen on the cathode in tests with a magnetic field as well as tests without the applied field, thus giving a cathode mass gain. Therefore, no cathode mass loss rates have been presented. Further testing is required to determine the feasibility of applying a magnetic field to an arcjet design.

Constricted Arc

Cathode mass loss. Figure 15 shows the LaB₆ cathode mass loss comparing constricted and unconstricted gas flow configurations. Tests were performed with both conventional and reverse flow patterns. With the conventional flow pattern (Fig. 15(a)) at 100 SCCM using a copper, water-cooled anode the LaB₆ mass loss in the constricted arc configuration was 6.7×10^{-5} g/min and no measurable mass loss was reported earlier in the unconstricted arc configuration. During the constricted arc tests, the voltage fluctuated from the 36 to 47 V. This instability may have been the result of the arc anode attachment moving from a point on the upstream face of the constrictor to

a point along the length of the constrictor. This arc instability may have caused the increase in cathode erosion.

A thoriated tungsten constrictor was also tried with the conventional flow pattern. At 100 SCCM, significant erosion of the anode occurred, even with water cooling, and a mass gain on the cathode was measured. This mass gain was due to deposits of tungsten from the anode. At 100 SCCM, the cathode mass loss was 1.3×10^{-4} g/min. At this flow rate, the voltage fluctuated between 35 and 50 V, possibly due to movement of the anode attachment to the low pressure region of the constrictor, on the downstream end of the insert. Again, the cathode mass loss may have been due to arc instability. The flow pattern through the inside of the LaB₆ tube may not have been optimum, possibly leading to some instability. For purposes of comparison a 0.32 diameter thoriated tungsten rod cathode was also tried. This cathode was ground flat on three sides to allow gas to flow over the cathode. At 4000 SCCM, the arc voltage fluctuated between 35 and 52 V and the cathode mass loss was 1×10^{-4} g/min. A more optimum flow pattern may have reduced arc instabilities and decreased erosion.

Figure 15(b) shows the cathode mass loss with reverse flow. At 100 SCCM, the cathode mass loss decreased by a factor of three using the constricted arc configuration. This reduction in mass loss may have been the result of cathode cooling as the cathode support structure required water cooling to prevent possible melting of the copper. Increasing the flow to 4000 SCCM reduced the erosion by approximately 15 percent, possibly due to a small film cooling effect. The arc voltages were 33±2 V and 36±2 V in the unconstricted and constricted arc configurations, respectively. The difference in voltage may have been due to cathode spot formation on the inside of the cathode tube.

Anode mass loss. Figure 16 shows the ThO₂-W anode mass loss for a constricted arc with conventional and reverse flow. As shown in Fig. 16(a), with a conventional flow pattern, the anode mass loss was 7.2×10^{-4} g/min at 100 SCCM and 1×10^{-4} g/min at 4000 SCCM. Figure 17 shows photographs of thoriated tungsten inserts after running for 300 min at 100 SCCM and at 4000 SCCM in nitrogen. At 100 SCCM melting of the upstream face of the anode was evident. At 4000 SCCM, localized melting did occur near the outer edge of the insert, but the melting was not as severe as in the test at 100 SCCM. It appears, therefore, that as flow increases erosion decreases.

In the free-burning arc tests at 100 SCCM, the anode mass loss was 3.77×10^{-4} g/min with conventional flow, which was lower than the mass loss in the constricted arc configuration at 100 SCCM. In the free-burning arc tests, however, the anode rod area was different than the area in the constricted arc, which had a nozzle-shaped anode. Because the areas were different, the heat transfer and evaporation of the anode were probably different, and the tests were not comparable. A separate test done with a free-burning arc configuration with a thoriated tungsten insert gave a mass loss of 7.2×10^{-4} g/min, which was the same

as that in the constricted arc configuration. At these flow rates it therefore appears that erosion was a function of geometry but not necessarily gas confinement.

A decrease in anode mass loss was found when the flow was increased from 100 to 4000 SCCM in the conventional flow design. This decrease in the mass loss may have been due to the random movement of the arc over the anode, or possibly arc formation in the low pressure "region" of the constrictor. As discussed above, arc movement has been found to decrease anode erosion. Random arc movement, however, may cause arc instabilities which could affect reliability and cathode mass loss. Therefore, at high flows in a constricted arc configuration there may be the conflicting effects of distributing the heat load over the anode and forming arc instabilities.

Vortex gas flow has been shown to stabilize the arc, and it may be possible to force the arc to seat downstream of the constrictor with vortex flow. By forcing the arc to attach in this low pressure region, the arc may be diffuse, evenly distributing the heat over the surface of the anode.³² Tests at the 2 kW power level with hydrogen⁴ showed some success at moving the arc toward the downstream end of the constrictor. During that 150 hr test, the anode attachment appeared to be in the divergent section of the nozzle, although it was apparent that the anode attachment changed often during the test. More work is required to determine if a diffuse anode attachment can be achieved consistently with storable propellants.

Figure 16(b) shows the anode mass loss with a reverse flow pattern. At 100 SCCM the mass loss rates in the constricted and unconstricted arcs were similar, indicating that the anode mass loss mechanisms may be the same in both configurations. A factor of 3 decrease in erosion was found when the flow was increased to 4000 SCCM. This reduction in erosion was the result of increased film cooling at higher flows. Although the reverse flow pattern decreased anode erosion the effects on arcjet energy efficiencies and arc stability are unclear. Further testing is required to determine the feasibility of a reverse flow arcjet design.

Current comparison. Figure 18 is a comparison of the electrode mass loss in a constricted arc at 10 and 20 A. The cathode mass loss for LaB₆ decreased from 5.8×10^{-5} g/min at 10 A to no measurable mass loss at 20 A. Thoriated tungsten also had a negligible cathode mass loss at 20 A in the reverse flow constricted arc configuration. This decrease in erosion may have been due to increased arc stability at 20 A, as evidenced by fewer voltage fluctuations. The anode mass loss increased by nearly one order of magnitude as the current was increased from 10 to 20 A. At higher currents the anode is subjected to a higher heat load, causing more evaporation than at lower currents. In the reverse flow design, as in the conventional flow design, it may be required to move the arc over the surface of the anode to prevent erosion, as was suggested by Greco and Stoner³³ in initial experiments with a reverse flow design. The arc voltage was 33±2 V at both 10 and 20 A.

Summary of Results

In an effort to reduce electrode erosion in low power arcjet thrusters, a study was conducted to characterize the mass loss of various electrode materials in a nitrogen arc. Lanthanum hexaboride and thoriated tungsten were found to have low cathode erosion rates when tested for 5 hr at 10 A. Although lanthanum hexaboride had a low mass loss rate this material exhibited some thermal stress cracking, especially upon repeated starts. Thoriated tungsten also had a low mass loss rate, but depletion of thorium may cause voltage fluctuations. Long-term tests (>100 hr) must be run to determine the optimum cathode material.

Thoriated tungsten and pure tungsten were found to have the lowest anode mass loss rates of the materials tested. Thoriated tungsten had a slightly higher mass loss rate than pure tungsten, but because of its machinability thoriated tungsten may be a more practical material.

Some possible options available to reduce electrode erosion include cooling the anode, reversing the gas flow direction, imposing an external magnetic field, and reducing the number of starts. In this study, all of these options were found to significantly decrease the electrode mass loss; however, the effects of each option on energy efficiency and arc stability are not known. Further research is required to determine the feasibility of incorporating anode cooling, reverse flow, and/or magnetic fields into an arcjet design.

Tests with a constricted arc design showed that arc stability may have a significant effect on electrode erosion. Arc instabilities may reduce cathode life. Previous studies have shown success in stabilizing the arc with vortex flow. Experimentation in this area is required to determine the effects of vortex flow stabilization on electrode erosion in low power arcjet thrusters.

References

1. Wallner, L.E. and Czika, J., Jr., "Arcjet Thruster for Space Propulsion," NASA TN-D-2868, July 1965.
2. John, R.R., Connors, J.F., and Bennett, S., "Thirty Day Endurance Test of a 30-kW Arcjet Engine," AIAA Paper 63-274, June 1963.
3. Todd, J.P. and Sheets, R.E., "Development of a Regeneratively Cooled 30 kW Arcjet Engine," AIAA Journal, Vol. 3, No. 1, Jan. 1965, pp. 122-126.
4. McCaughey, O.J., Geiderman, W.A., Jr., and Miller, K.: "Research and Advanced Development of a 2 kW Arcjet Thruster," Plasmadyne Corp., Santa Ana, CA, July 1963. (NASA CR-54035)
5. Meltzer, J., Chen, C.J., Greco, R., McKenna, Q., Mitcheltree, G., Price R., and Stoner W., "Properties of Plasmas as They Pertain to Thermal Arcjets," Aeronautical Systems Division ASD-TDR-62-451, Aug. 1962.
6. Jack, J.R., "Theoretical Performance of Propellants Suitable for Electrothermal Jet Engines," NASA TN-D-682, 1962.
7. Farrel, G.A.: "Vacuum Arcs and Switching," IEEE Proceedings, Vol. 61, No. 8, Aug. 1973, pp. 1113-1136.
8. Kimblin, C.W., "Erosion and Ionization in the Cathode Spot Regions of Vacuum Arcs," Journal of Applied Physics, Vol. 44, No. 7, July 1973, pp. 3074-3081.
9. Daadler, J.E., "Cathode Erosion of Metal Vapor Arcs in Vacuum," Doctoral Thesis, Eindhoven University of Technology, The Netherlands, 1978.
10. Kimblin, C.W., "Cathode Spot Erosion and Ionization Phenomena in the Transition from Vacuum to Atmospheric Pressure Arcs," Journal of Applied Physics, Vol. 45, No. 12, Dec. 1974, pp. 5235-5244.
11. Cobine, J.D. and Burger, E.E., "Analysis of Electrode Phenomena in the High Current Arc," Journal of Applied Physics, Vol. 26, No. 7, July 1955, pp. 895-900.
12. Hardy, T.L., and Nakanishi, S., "Cathode Degradation and Erosion in High Pressure Arc Discharges," 17th International Electric Propulsion Conference, Japan Society for Aeronautical and Space Sciences, 1984, pp. 560-573.
13. Lafferty, J.M., "Boride Cathodes," Journal of Applied Physics, Vol. 22, No. 3, Mar 1951, pp. 299-309.
14. Wolski, W., "Press Sintered Hexaboride Cathodes," Royal Institute of Technology, NP-18432 REPT-69-12, May 24, 1969.
15. Masser, P.S., "Recent Experimental Plasmajet Thruster Results," AIAA Journal, Vol. 1, No. 6, July 1963, pp. 1651-1652.
16. Adams, R.P., Copeland, M.I., Deardorff, D.K., and Lincoln, R.L., "Cast Hafnium Carbide-Carbon Alloys," U.S. Bureau of Mines, Dept. of Interior, Report of Investigations, Report BM-RI-7137, June 1968.
17. Finkelnburg, W., and Maecker, H., "Electric Arcs and Thermal Plasma," Union Carbide Corp., ARL-62-302, Jan. 1962.
18. Cobine, J.D., "Gaseous Conductors," Dover Publications, New York, 1958, p. 292.
19. Cobine, J.D., "Gaseous Conductors," Dover Publications, New York, 1958, p. 293.
20. Semenova, O.P., and Petrova, M.V., "Influence of An Atmosphere of Argon, Nitrogen, or Air on the Emission of An Arc Discharge," Bulletin of the Academy of Sciences (USSR), Vol. 26, No. 7, 1962, pp. 950-953.

21. Futamoto, M., Nakazawa, M., Usami, K., Hosoki, S., and Kawake, U.: "Thermionic Emission Properties of a Single-Crystal La₈₆Cathode," *Journal of Applied Physics*, Vol. 51, No. 7, July 1980, pp. 3869-3876.
22. Harry, J.E., "The Measurement of the Erosion Rate at the Electrodes of an Arc Rotated by a Transverse Magnetic Field," *Journal of Applied Physics*, Vol. 40, No. 1, Jan. 1969, pp. 265-270.
23. John, R.R., Mironer, A., Macomber, H., and Cournes, J.F., "Arcjet Engine Performance - Experiment and Theory II," *ARS Paper* 61-101-1795, 1961.
24. Holm, R., "The Vaporization of the Cathode in the Electric Arc," *Journal of Applied Physics*, Vol. 20, July 1949, pp. 715-716.
25. Neurath, P.W. and Gibbs, T.W., "Arc Cathode Emission Mechanisms at High Currents and Pressures," *Journal of Applied Physics*, Vol. 34, No. 2, Feb. 1963, pp. 277-283.
26. Schneider, P., "Thermionic Emission of Thoriated Tungsten," *Journal of Chemical Physics*, Vol. 28, No. 4, April 1958, pp. 675-682.
27. Bade, W.L. and Yos, J.M., "Theoretical and Experimental Investigation of Arc Plasma-Generation Technology," Part II-Applied Research on Electric Arc Phenomena, Vol. 1, ASD-TDR-62-729, Pt. II, Vol. 1, Sept. 1963.
28. Samsonov, G.V., "Properties Index," Plenum Press Handbooks of High Temperature Materials, Vol. 2, Plenum Press, New York, 1964.
29. Forman, R., "A Proposed Physical Model for the Impregnated Tungsten Cathode Based on Auger Surface Studies of the Ba-O-W System," *Applications of Surface Science*, Vol. 2, No. 2, Jan., 1979, pp. 258-274.
30. Boldman, D.R., Shepard, C.E., and Fahan, J.C.: "Electrode Configurations for a Wind-Tunnel Heater Incorporating the Magnetically Spun Electric Arc," NASA TN-D-1222; 1962.
31. Ducati, A.C., Jahn, F.G., Mahlberger, E., and Treat, R.P., "Design and Development of a Thermionic Electric Thrustor," Giannini Scientific Corp., Santa Ana, CA, FR-056-968, May 1966. (NASA CR-54703)
32. Kimblin, C.W., "Anode Phenomena in Vacuum and Atmospheric Pressure Arcs," *IEEE Transactions on Plasma Science*, Vol. PS-2, No. 4, Dec. 1974, pp. 310-319.
33. Greco, R.V. and Stoner, W.A., "Research and Development of a 1-kW Plasmajet Thruster," *AIAA Journal*, Vol. 1, No. 2, Feb. 1963, pp. 320-324.

ORIGINAL PAGE IS
OF POOR QUALITY

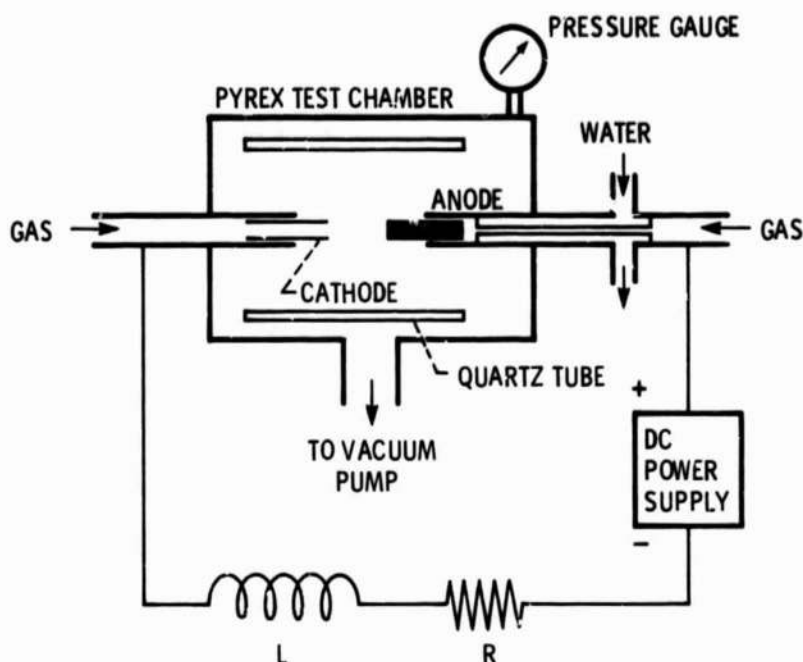


Figure 1. - Arcjet electrode experimental system.

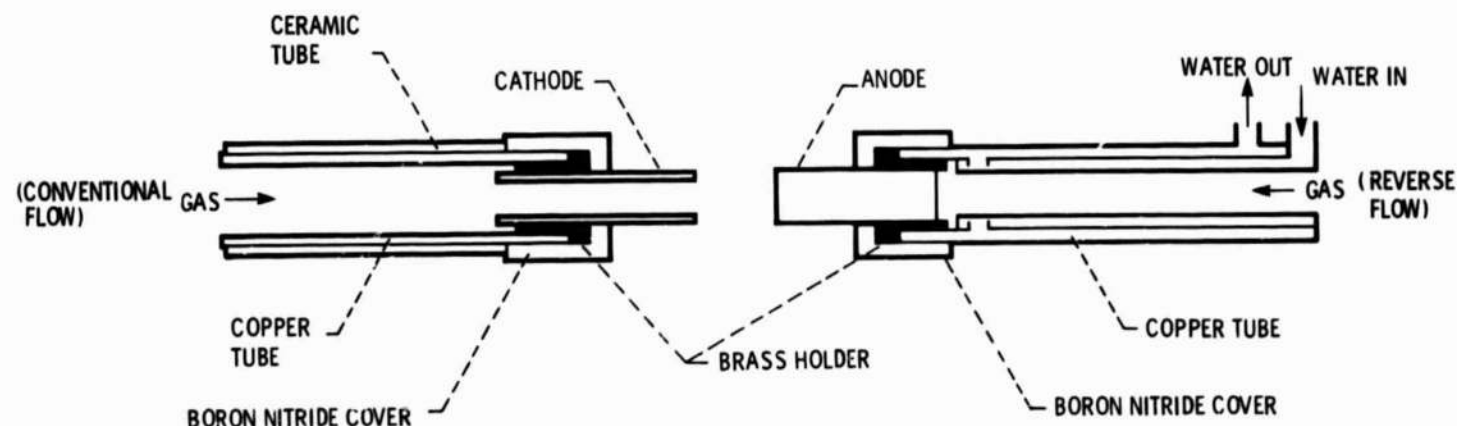


Figure 2. - Free-burning arc configuration.

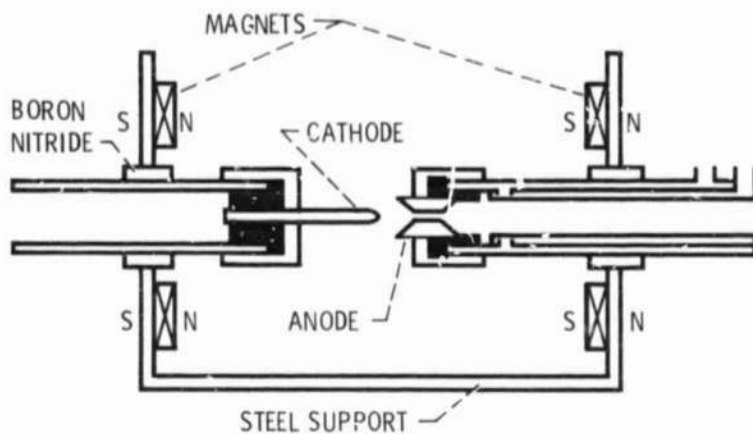


Figure 3. - Axial magnetic field configuration, (top view.)

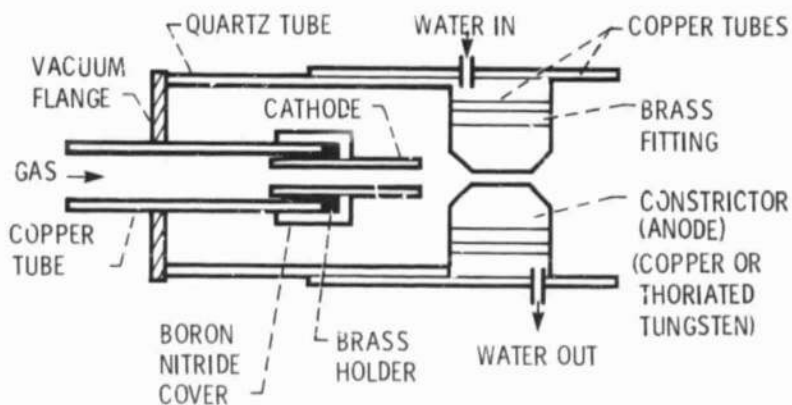


Figure 4. - Constricted arc configuration, conventional flow.

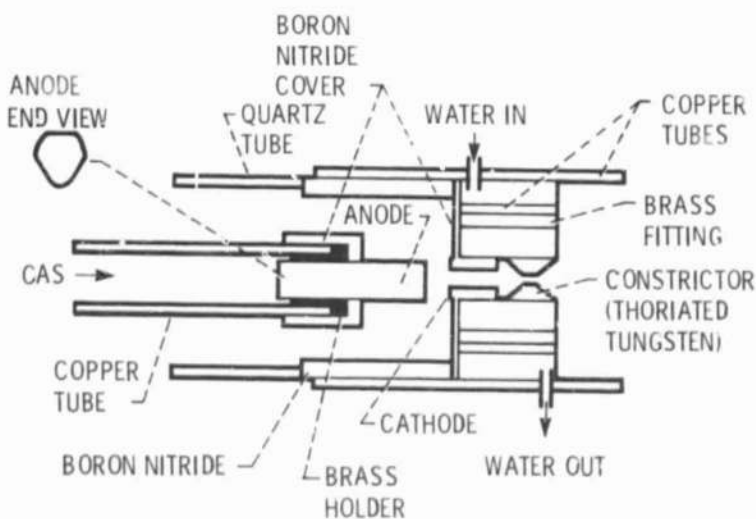
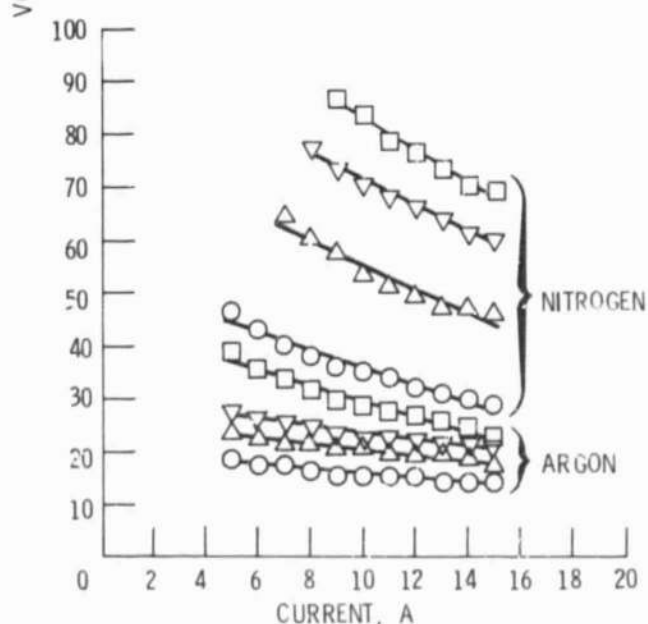
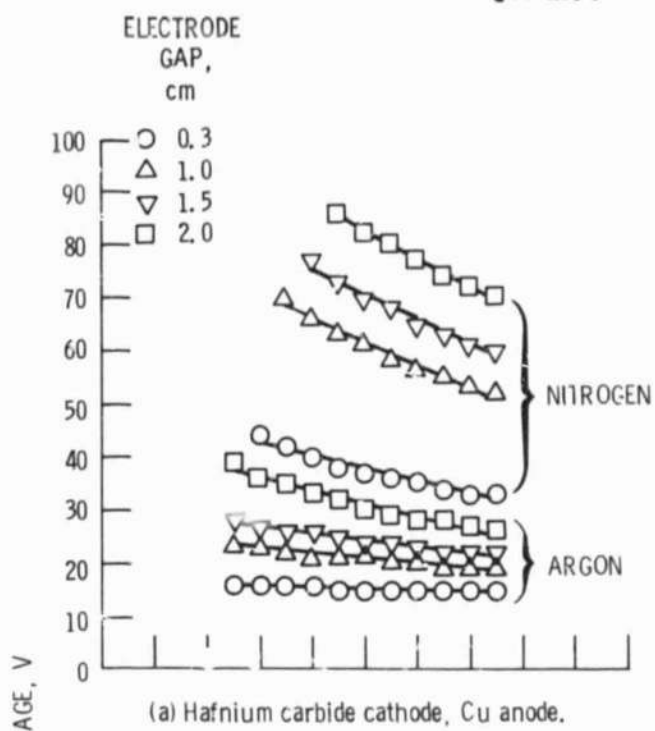


Figure 5. - Constricted arc configuration, reverse flow.

ORIGINAL PAGE IS
OF POOR QUALITY



(b) Lanthanum hexaboride cathode, Cu anode.

Figure 6. - Voltage-current characteristics, free
burning arc. 10 A; 100 sccm; 760 torr.

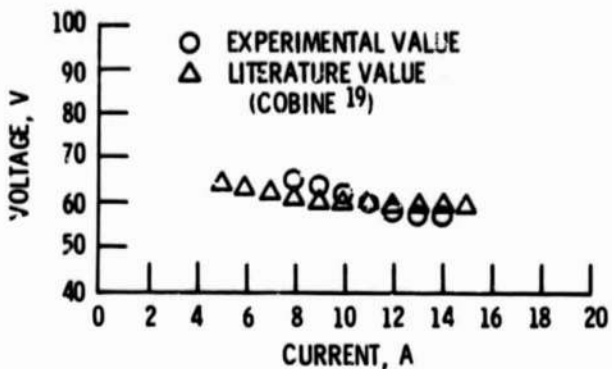


Figure 7. - Arc characteristic comparison, free-burning arc. Graphite cathode, anode. 10 A; 100 sccm; 760 torr; 0.3 cm gap.

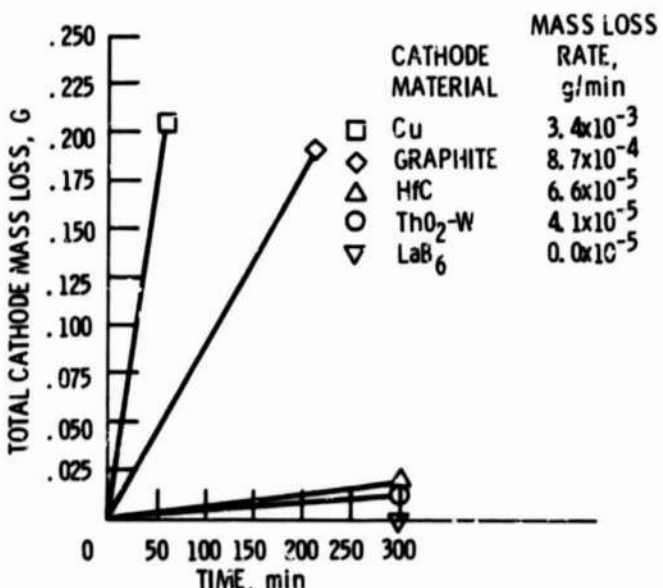


Figure 8. - Cathode materials mass loss comparison, free-burning arc. 10 A; 100 sccm; 760 torr; 0.3 cm gap, Cu water-cooled anode.

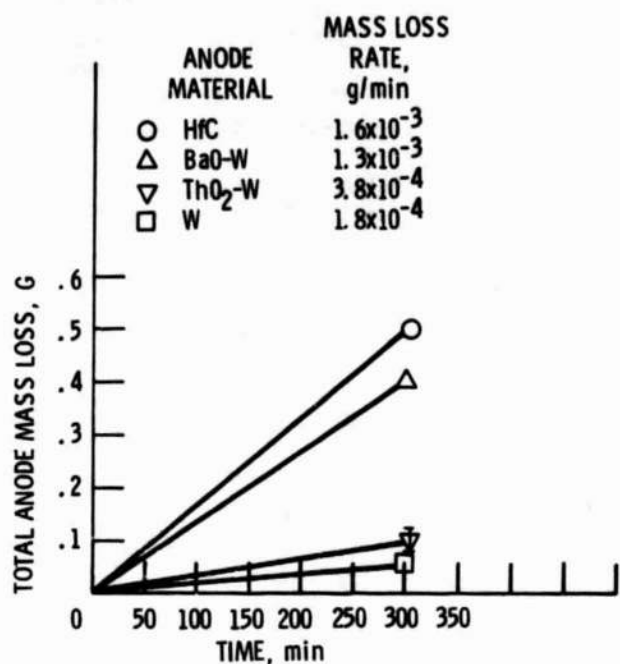


Figure 9. - Anode materials mass loss comparison, free-burning arc. LaB₆, cathode; 10 A; 100 sccm; 760 torr; 0.3 cm gap.

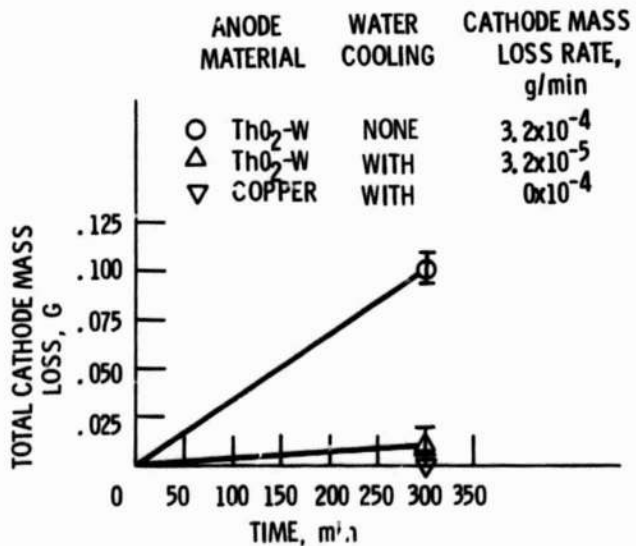


Figure 10. - Anode water cooling effects on cathode mass loss, free-burning arc. LaB₆ cathode; 10 A; 100 sccm; 760 torr; 0.3 cm gap.

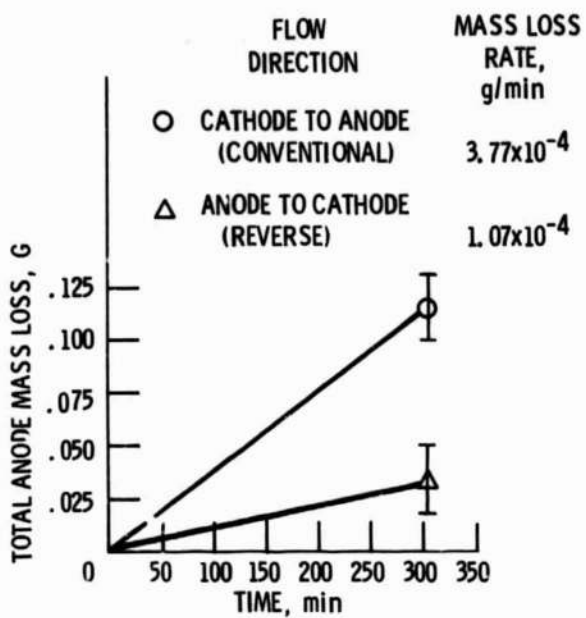


Figure 11. - Flow direction effects on anode mass loss, free-burning arc.
 LaB_6 cathode; $\text{ThO}_2\text{-W}$ anode; 10 A;
 100 sccm; 760 torr; 0.3 cm gap.

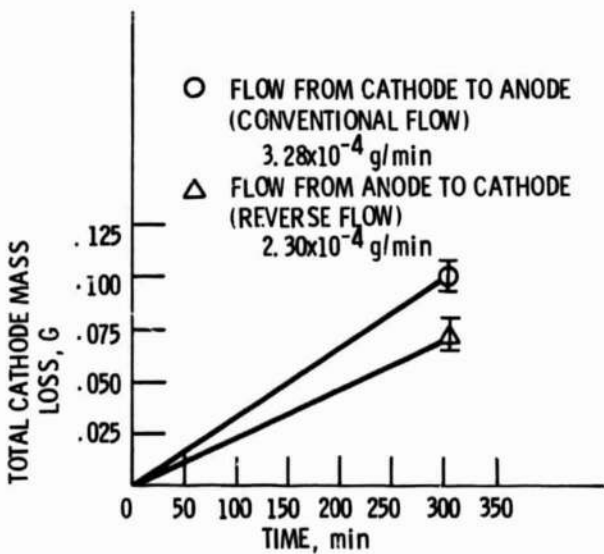


Figure 12. - Flow direction effects on cathode mass loss, free burning arc.
 LaB_6 cathode; $\text{ThO}_2\text{-W}$ anode;
 10 A; 100 sccm; 760 torr; 0.3 cm
 gap.

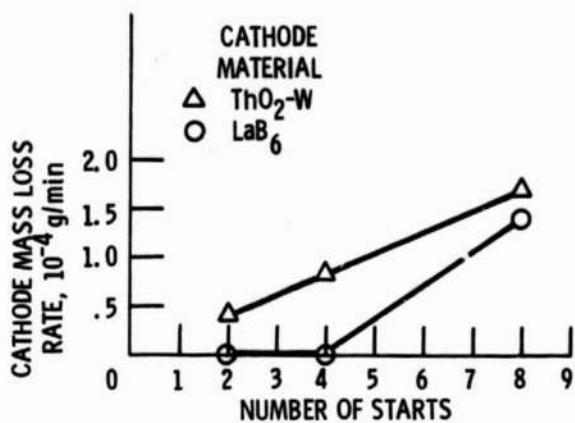


Figure 13. - Effect of the number of starts on cathode mass loss, free-burning arc, Cu water-cooled anode, 10 A; 100 sccm; 760 torr; 0.3 cm gap.

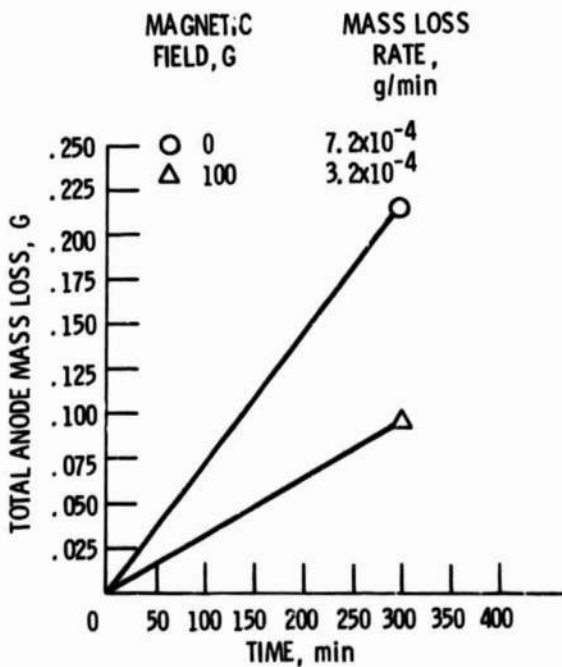


Figure 14. - Magnetic field test, free-burning arc. ThO₂-W cathode; ThO₂-W water-cooled anode; 10 A; 100 sccm; 0.3 cm gap.

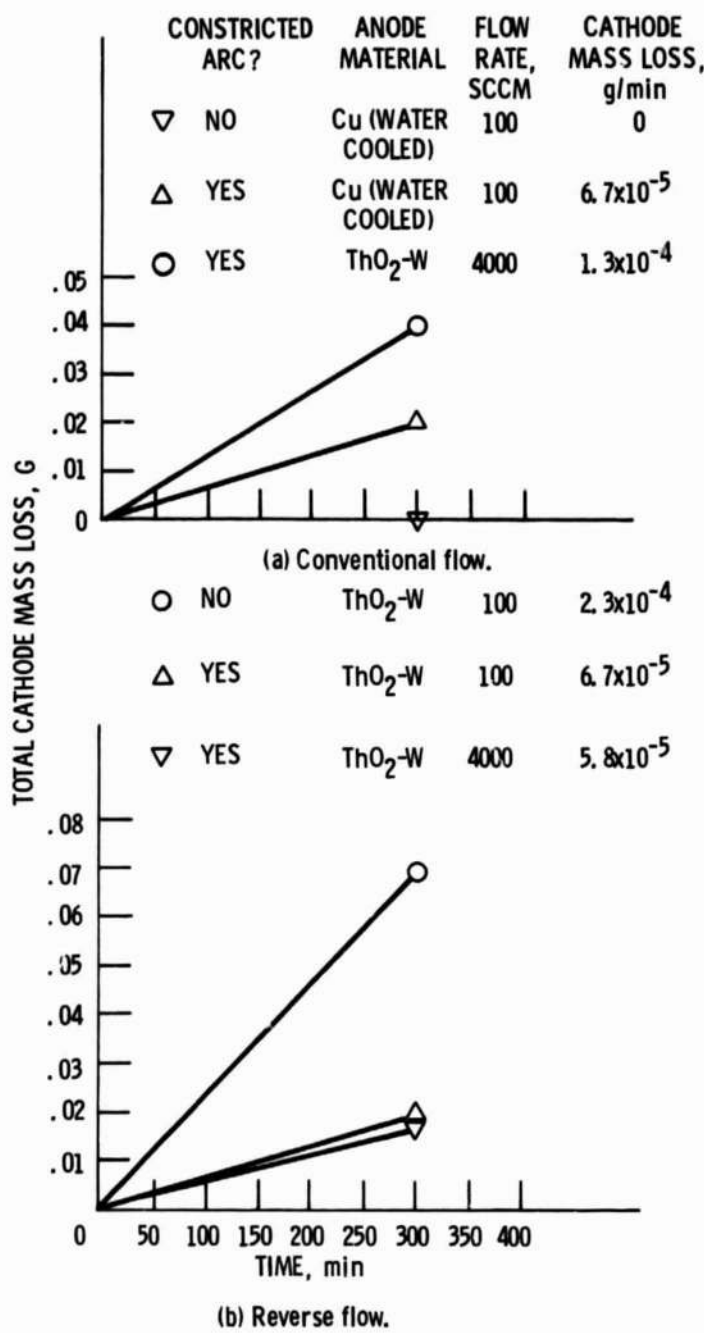


Figure 15. - Effect of gas flow constriction
on cathode mass loss. 10 A; 0.3 cm
gap; LaB_6 cathode.

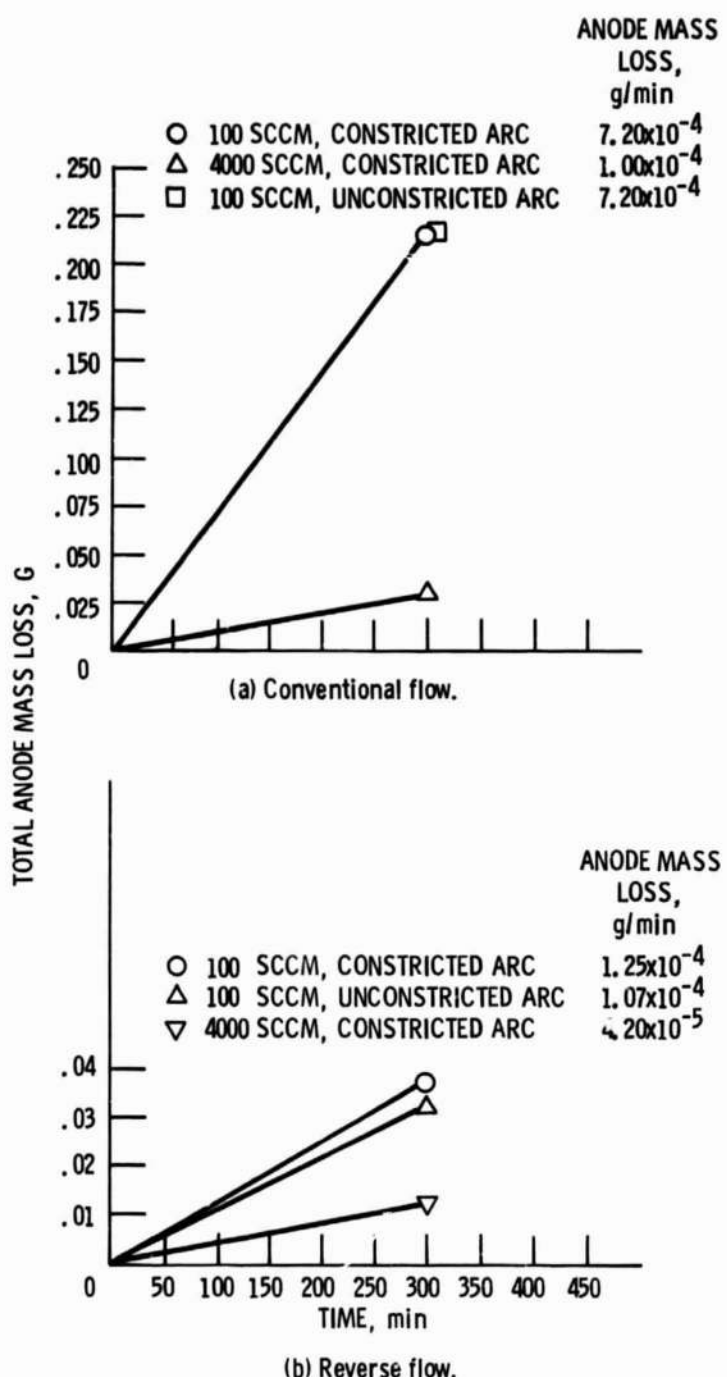
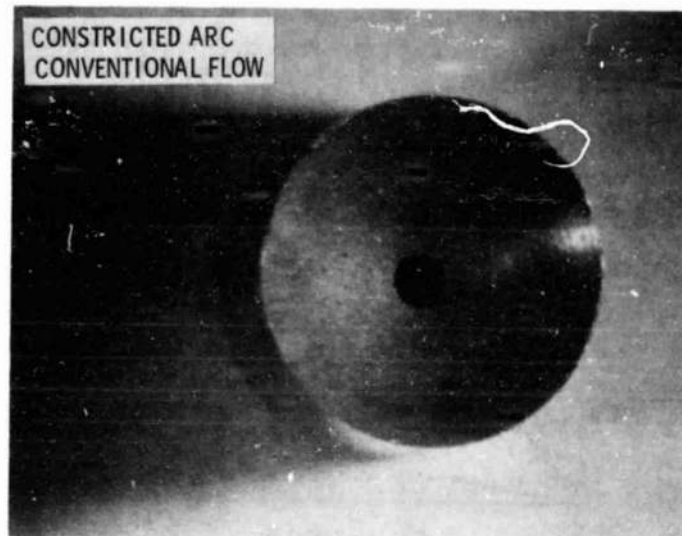
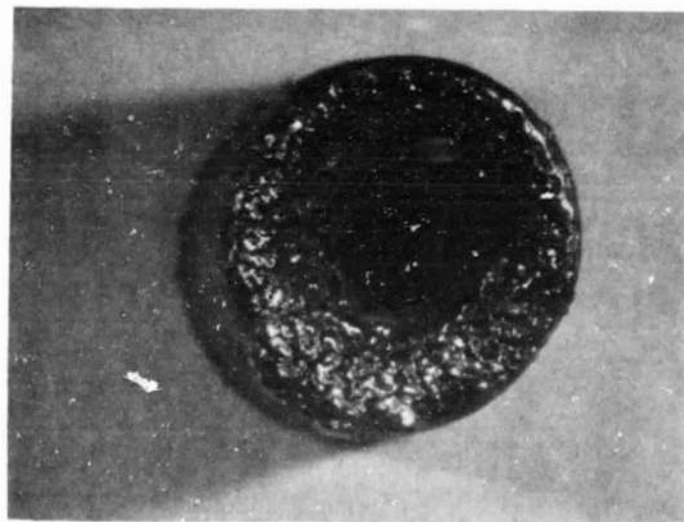


Figure 16. - Effect of gas flow constriction on anode mass loss. 10 A; 0.3 cm gap; LaB_6 cathode.

ORIGINAL PAGE IS
OF POOR QUALITY



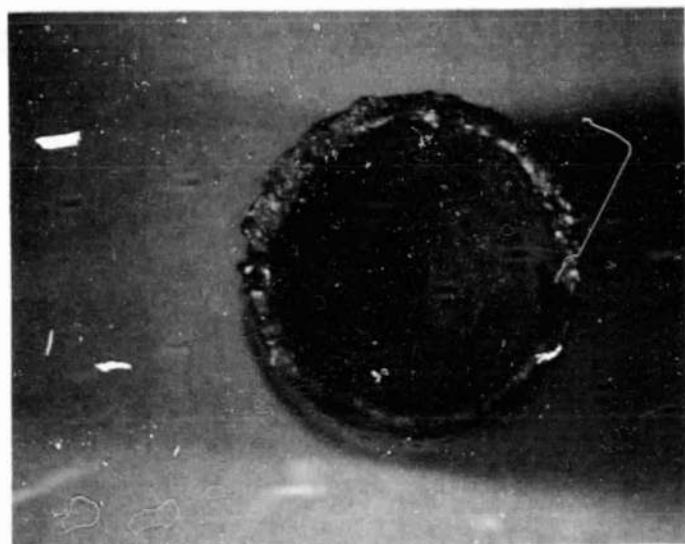
(a) Before running in nitrogen.



(b) After running in nitrogen at 100 SCCM.

Figure 17. - Typical thoriated tungsten anode insert.

ORIGINAL PAGE IS
OF POOR QUALITY



(c) After running in nitrogen at 4000 SCCM.

Figure 17. - Concluded.

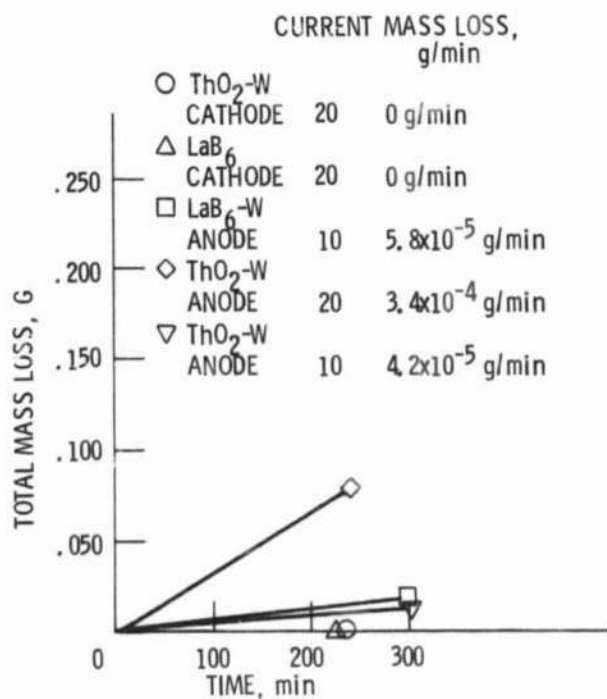


Figure 18. - Effect of current
on electrode mass loss for
the constricted arc con-
figuration, 4000 sccm;
0.3 cm gap; reverse flow,
water-cooled cathode.

1. Report No. NASA TM-87087	2. Government Accession No.	3. Recipient's Catalog No.	
4. Title and Subtitle Electrode Erosion in Arc Discharges at Atmospheric Pressure		5. Report Date	
		6. Performing Organization Code 506-55-22	
7. Author(s) Terry L. Hardy		8. Performing Organization Report No. E-2673	
		10. Work Unit No.	
9. Performing Organization Name and Address National Aeronautics and Space Administration Lewis Research Center Cleveland, Ohio 44135		11. Contract or Grant No.	
		13. Type of Report and Period Covered Technical Memorandum	
12. Sponsoring Agency Name and Address National Aeronautics and Space Administration Washington, D.C. 20546		14. Sponsoring Agency Code	
15. Supplementary Notes Prepared for the 18th International Electric Propulsion Conference cosponsored by the AIAA, JSASS, and DGLR, Alexandria, Virginia, September 30 - October 2, 1985.			
16. Abstract An experimental investigation was performed in an effort to measure and increase lifetime of electrodes in an arcjet thruster. The electrode erosion of various anode and cathode materials was measured after tests in an atmospheric pressure nitrogen arc discharge at powers less than 1 kW. A free-burning arc configuration and a constricted arc configuration were used to test the materials. Lanthanum hexaboride and thoriated tungsten had low cathode erosion rates while thoriated tungsten and pure tungsten had the lowest anode erosion rates of the materials tested. Anode cooling, reverse gas flow, and external magnetic fields were all found to reduce electrode mass loss.			
17. Key Words (Suggested by Author(s)) Cathodes; Electrodes; Erosion; Nitrogen; Tungsten; Lanthanum hexaboride		18. Distribution Statement Unclassified - unlimited STAR Category 20	
19. Security Classif. (of this report) Unclassified	20. Security Classif. (of this page) Unclassified	21. No. of pages	22. Price*